national accelerator laboratory

NAL-PUB-73/46-THY

July 1973

Patterns of Diffractive Production

D. HORN[†]
National Accelerator Laboratory
P. O. Box 500, Batavia, Illinois 60510

and

M. MOSHE[*†]
California Institute of Technology
Pasadena, California 91109

ABSTRACT

We discuss diffractive production in the context of two-component models. After defining the class of models that we consider and discussing their general properties, we develop integral equations for the generating functions of diffractive processes. We consider single and double diffraction and two fireball production. We investigate the behavior of the partial cross-sections for n-particle production in all three cases and obtain a successful fit to recent data.

---

[*]Work supported in part by the U.S. Atomic Energy Commission.

Prepared under Contract AT(11-1)-68 for the San Francisco Operations Office, U.S. Atomic Energy Commission.

[†]On leave of absence from Tel-Aviv University, Tel-Aviv, Israel.

I. THE TWO-COMPONENT MODEL

Let us start the discussion of this model by defining a "proper" production amplitude as any amplitude which cannot be separated into two disconnected parts by the elimination of a Pomeron exchange. We use the word Pomeron to refer to any j-plane singularity which passes through (or very near to) $j = 1$ at $t = 0$. The proper amplitude does not have any such singularity in any t-channel.

The main assumption of the two-component model* is that the sum of all proper contributions to the s-channel unitarity equation builds up a Pomeron exchange (as well as lower exchanges) in two-body scattering. This is symbolically shown in Fig. 1. We use the open ellipse to designate a proper production amplitude, and the wiggly line to represent Pomeron exchange.

Improper production amplitudes can also be referred to as diffractive mechanisms since they involve Pomeron exchanges. Three such amplitudes are shown in Fig. 2, and their corresponding contributions to s-channel unitarity are shown in Fig. 3. The unitarity equation can be written symbolically in the form of Fig. 4 where we showed explicitly the elastic and proper contributions. The remaining diffractive productions build up the rest of this equation. Some such terms were shown in Fig. 3 and many more exist. Examples are more iterations of Pomerons, or replacement of some Pomerons in Fig. 3 by lower lying trajectories.

Thus Fig. 3I shows a triple-Pomeron[2] contribution which we may denote by PPP. If one chooses a non-leading component in the proper production amplitude one has a non-scaling diffractive term PPR (where R denotes a non-Pomeron Regge singularity). Such a term has to be added to Fig. 4 under the general diffractive category. Moreover, whereas an RRP term is already included in the proper contribution (Fig. 1), we should not forget that interference terms such as PRP can also occur and we add them to the general diffractive category.

The first question one may now ask is whether the various wiggly lines, that we called Pomerons, refer always to the same object. In general that must not be the case and we may conceive of different j-plane singularities building up the diagrams of Fig. 3. It is however easier, and perhaps also more appealing, to assume that all of them are the same moving pole. This leads to well known problems[3] since further iterations of Pomeron exchanges will lead to violations of the Froissart bound. One way out[4,5] is to assume that the pole generated by the proper amplitudes, Fig. 1, lies below j=1 at t=0. Then one interprets the diagrams of Fig. 3 as involving two different Regge poles - one representing the sum of proper contributions and the other is the "true" Pomeron, defined by the unitarity equation, which turns out to lie above the original moving pole at $t = 0$. An alternative approach is to concede that the assumption of a Pomeron pole at $j = 1$ is wrong but to use it nonetheless as an approximation.**

Thus we may interpret Fig. 2I as representing a triple-Pomeron pole together with the sum of all possible absorptive cut corrections. If however the absorptive correction is small,[6] the approximation of this amplitude by the triple-Pomeron pole term follows.

We will not try to build a complete and consistent theory of diffraction. Our interest lies in investigating the expected structure of diffractive distributions for the three different cases of Fig. 2. In the equations which we develop in the following section we use the Pomeron pole approximation in order to obtain explicit results. Their modifications for other kinds of factorizable singularities are straightforward. In more general cases the corrections can become more complicated and change the structure of our integral equations.

II. DIFFRACTIVE GENERATING FUNCTIONS

In the present chapter we develop formulas for the generating functions of the diffractive production processes in Fig. 2. The generating functions are defined by

$$Q(s, z) = \sum_n z^n \sigma_n(s) \tag{1}$$

where $Q(s, z=1) = \sigma(s)$ is the contribution of a particular mechanism to the total cross-section. n designates the number of particles produced. We will use throughout the paper the longitudinal strong ordering description of the production processes. The particles are assumed to have low transverse momenta and the (invariant-mass)^2 of the various amplitudes are defined in Fig. 2. For case I - the triple Pomeron - we can then write

$$Q_I(s, z) = \frac{z}{\pi s} \int_1^s ds_1 \, B_I\left(\frac{s}{s_1}\right) \bar{Q}(s_1, z) \tag{2}$$

$\bar{Q}$ is the generating function for the sum of proper amplitudes of Fig. 2(I) from which we eliminate the triple Pomeron coupling g(t). Thus the Pomeron-particle cross-section is $g(t)\bar{Q}(s, z=1) = g(t)\bar{\sigma}(s)$. This coupling g(t) is included in B_I. Using a pole approximation one can write

$$B_I(s) = \frac{1}{16\pi s} \int dt \, s^{2+2\alpha' t} \left|\beta(t)\right|^2 g(t) \tag{3}$$

where $\beta(t)$ includes the coupling of the Pomeron to the external particle and the signature factors. Using a parameterization

$$|\beta(t)| = \beta e^{bt} \qquad g(t) = g\, e^{ct} \tag{4}$$

one obtains the result

$$B_I(s) = \frac{s}{16\pi}\,\beta^2\, g\,\frac{1}{2\alpha' \ln s + 2b+c} \tag{5}$$

and the equation for Q_I reduces to

$$Q_I(s,z) = \frac{z\beta^2 g}{16\pi^2}\int_1^s \frac{ds_1}{s_1}\,\frac{\bar{Q}(s_1,z)}{2b+c+2\alpha' \ln(\frac{s}{s_1})} \tag{6}$$

A more elaborate derivation of the integral equations for cases I-III is given in the Appendix in which we show how they can be incorporated in the multiperipheral model. We use a dimensionless notation (in scales of $s_0 = 1\ \mathrm{GeV}^2$) and we suppress also factors of m_T^2 that appear in rapidity definitions. Thus denoting $Y = \ln s$, $y_1 = \ln s_1$, we see that Eq. (6) is an integral over y_1 leading to a cross-section of the form

$$\begin{aligned} \sigma_I &= \frac{\beta^2 g\bar{\sigma}}{16\pi^2}\,\frac{1}{2\alpha'}\ln\left(1+\frac{2\alpha'}{2b+c}\,Y\right) && \alpha' \neq 0 \\ &= \frac{\beta^2 g\bar{\sigma}}{16\pi^2}\,\frac{Y}{2b+c} && \alpha' = 0 \end{aligned} \tag{7}$$

for the Pomeron pole model. This is the well-known triple Pomeron result.[2]

Using the same assumptions and techniques it is straightforward to write the equations for the other cases. In case II - the "two jets" production - we find

$$Q_{II} = \frac{1}{\pi^2 s}\int_1^s\int_1^s \theta(s-s_1 s_2)\, B_{II}\left(\frac{s}{s_1 s_2}\right) ds_1 ds_2\, \bar{Q}(s_1,z)\,\bar{\bar{Q}}(s_2,z) \quad (8)$$

Strong ordering implies $s > s_1,\ s_2,\ \frac{s}{s_1 s_2} > 1$. The integrations on s_1 and s_2 in Eq. (8) are carried out over the whole region $1 < s_1, s_2 < s$ subject to the condition $s/s_1 s_2 > 1$. It is important to note that in the derivation of the analogous integral equation for the multiperipheral model with only one exchange (see Appendix) we have to limit the range of integration to non-overlapping regions of rapidity, e.g., $0 < \ln s_{1,2} < \frac{1}{2}\ln s$ in order to avoid counting the same diagram several times. In Eq. (8), however, $\bar{Q}$ represents the sum of proper amplitudes which do not involve Pomeron exchanges, as postulated in the beginning of our discussion. Hence no multiple counting equestion arises and the integration has to be carried out over the whole range described above.

Using a conventional Regge pole representation one finds

$$B_{II}(s) = \frac{1}{16\pi s}\int dt\, s^{2+2\alpha' t}\, g^2(t) = \frac{s}{16\pi}\,\frac{g^2}{2\alpha' \ln s + 2c} \quad (9)$$

Hence one obtains the equation

$$Q_{II} = \frac{g^2}{16\pi^3}\iint \theta(s-s_1 s_2)\,\frac{ds_1}{s_1}\,\frac{ds_2}{s_2}\,\frac{1}{2\alpha' \ln\frac{s}{s_1 s_2} + 2c}\,\bar{Q}(s_1,z)\bar{Q}(s_2,z) \quad (10)$$

and the solution

$$\sigma_{II} = \frac{g^2\bar{\sigma}^2}{16\pi^3}\left[\frac{1}{(2\alpha')^2}\left(2c+2\alpha' Y\right)\ln\left(1+\frac{\alpha'}{c}Y\right) - \frac{Y}{2\alpha'}\right]$$

$$\xrightarrow[Y \gg 1]{} \begin{cases} \dfrac{g^2\bar{\sigma}^2}{16\pi^3}\,\dfrac{1}{2\alpha'}\,Y \ln\left(1+\dfrac{\alpha'}{c}Y\right) & \alpha' \neq 0 \\ \dfrac{g^2\bar{\sigma}^2}{16\pi^3}\,\dfrac{1}{4c}\,Y^2 & \alpha' = 0 \end{cases} \qquad (11)$$

Similarly one obtains for the double diffractive production - case III - the equation

$$Q_{III} = \frac{z^2}{\pi^2 s^2}\iint \theta(s_1 s_2 - s)\, ds_1\, ds_2\, B_I\left(\frac{s}{s_1}\right) B_I\left(\frac{s}{s_2}\right) \bar{\bar{Q}}\left(\frac{s_1 s_2}{s}, z\right) \qquad (12)$$

Here B_I are the same functions that occur in case I. However $\bar{\bar{Q}}$ refers now to a Pomeron-Pomeron production process. As before, the triple Pomeron coupling, g(t), is included in B_I. Therefore $\bar{\bar{Q}}\left(\frac{s_1 s_2}{s}, z=1\right)$ equals 1 in the case of a pole singularity. In this case B_I is given by Eq. (5), and Eq. (12) turns into

$$Q_{III} = \frac{z^2}{\pi^2}\,\frac{\beta^4 g^2}{(16\pi)^2}\iint \frac{ds_1}{s_1}\,\frac{ds_2}{s_2}\,\theta(s_1 s_2 - s)\,\frac{1}{2\bar{\alpha}'\ln\frac{s}{s_1}+2b+c}\cdot$$

$$\cdot\,\frac{1}{2\alpha'\ln\frac{s}{s_2}+2b+c}\,\bar{\bar{Q}}\left(\frac{s_1 s_2}{s}, z\right) \qquad (13)$$

The contribution of double diffraction to the total cross-section will then be

$$\sigma_{III} = \frac{\beta^4 g^2}{(16\pi^2)^2} \, I(\ln s) \tag{14}$$

where

$$I(Y) = \int_0^Y dy_1 \int_{Y-y_1}^{Y} dy_2 \, \frac{1}{2b+c+2\alpha'(Y-y_1)} \, \frac{1}{2b+c+2\alpha'(Y-y_2)} \tag{15}$$

$$< \frac{Y}{2\alpha'(2b+c)} \ln\left(1 + \frac{2\alpha'}{2b+c} Y\right)$$

In the case of $\alpha' = 0$ one finds $I(Y) = \frac{Y^2}{2(2b+c)^2}$.

Let us turn now to a numerical estimate of the value of the various cross-sections. We will use for simplicity the case of a fixed pole ($\alpha' = 0$). It may be safely assumed that a calculation of a moving pole with small α' will give similar effective results as long as Y is not too big (see Fig. 5 below for a comparison between calculations with $\alpha' = .3$ and $\alpha' = 0$). From the equations developed above we find, for $\alpha' = 0$,

$$\sigma_I = \frac{\beta^2 g \bar{\sigma}}{16\pi^2} \frac{Y}{2b+c} \qquad \sigma_{II} = \frac{g^2 \bar{\sigma}^2}{16\pi^3} \frac{Y^2}{4c} \qquad \sigma_{III} = \frac{\beta^4 g^2}{(16\pi^2)^2} \frac{Y^2}{2(2b+c)^2} \tag{16}$$

All these expressions grow with ln s whereas the Pomeron pole of Fig. 1 leads to a constant contribution. If one nevertheless assumes that this constant represents the main bulk of non-diffractive (proper) cross-sections we may write

$$\sigma_{n.d} \approx \beta^2 \qquad \sigma'_{el} \approx \frac{\beta^4}{16\pi} \frac{1}{4b} \tag{17}$$

where σ'_{el} is the contribution of the proper amplitudes to σ_{el}. Using pp data[9] in the neighborhood of $s \approx 1000\ GeV^2$ we take $\sigma_{n.d.} \approx 30$ mb and $b \approx 2.5\ BeV^{-2}$. Equation (17) implies then $\beta \approx 8.8\ BeV^{-1}$. If we further assume that $\bar{\sigma} = \beta$, $c \approx b$ and choose $\sigma_I \approx 2.5$ mb we find that $\sigma_{II} \approx 0.8$ mb and $\sigma_{III} = \sigma_I^2/2\bar{\sigma}^2 \approx 0.1$ mb. Both values are pretty small. Note though that σ_{II} depends on the value of c for which we have no theoretical estimate. The choice c=b is arbitrary and σ_{II} can be increased considerably by letting $c << 1$. However in such a case the corresponding amplitude will contribute significantly to high t values. This may clash with the assumption of low transverse momenta which we implicitly used throughout the discussion. Hence the formulas have to be modified in a model dependent way in the case of strong two-jet production.

It is important to note that a fixed pole model cannot be continued to the next order in g since further couplings of the Pomeron will violate the Froissart bound. Hence we cannot regard such a fixed pole Pomeron as the true result. One may now ask if this situation can be remedied in a moving pole case. Looking at σ_I we realize that the energy behavior is now modified into a ln ln s increase. This may be further modified if the coupling g(t) vanishes at $t = 0$.[2] Thus choosing $g(t) = -tge^{ct}$ equation (6) will change according to $Q_I \to -\frac{\partial}{\partial c} Q_I$ and σ_I will have a finite limit

$$\sigma_I \to \frac{\beta^2 g\bar{\sigma}}{16\pi^2} \frac{1}{2\alpha'(2b+c)} \tag{18}$$

σ_{II} can be calculated in a similar fashion by changing $Q_{II} \to \frac{1}{4}\frac{\partial^2}{\partial c^2} Q_{II}$ and the result is still increasing like ln s:

$$\sigma_{II} \to \frac{g^2\bar{\sigma}^2}{16\pi^3} \frac{Y}{8\alpha' c^2} \tag{19}$$

The analogous modification of σ_{III} turns out to be

$$\sigma_{III} \to \frac{g^2\beta^4}{(16\pi^2)^2} \frac{1}{[2\alpha'(2b+c)]^2} \tag{20}$$

Thus we see that the vanishing triple-Pomeron coupling changes the behavior of σ_I and σ_{III} to constants. However σ_{II} continues to grow with ln s. This result is characteristic of the two component approach. As a matter of fact higher iterations of the Pomeron lead to corresponding higher Y powers thus rendering such a theory of simple poles invalid. Summing a series of such ln s power terms (in the leading log approximation) one obtains for the two body scattering amplitude a leading singularity which is higher than the original pole.[5,6] In view of the smallness of σ_{II} one may expect this correction to be very small, and so it is in the model of Ref. 5 which starts with a pole below j = 1. As we already mentioned above we do not try to develop a complete theory of the Pomeron. Rather we would like to use the pole picture as an approximation in order to derive (in the next section) some information about the expected partial cross-sections. Although we will use the pole

formulas developed above, we will keep in mind the possibility of logarithmic corrections.

Finally we would like to mention that not only decreasing cuts are possible but also higher singularities like double and triple poles at $j = 1$. Such singularities could be factorizable and would in this case fit into our formalism. If each Pomeron in Fig. 2 has an associated increase like $(\ln s)^{n_i}$ we should obtain

$$\sigma_I \sim (\ln s)^{\sum_i n_i + 1} \qquad \sigma_{II} \sim (\ln s)^{\sum_i n_i + 2} \qquad \sigma_{III} \sim (\ln s)^{\sum_i n_i + 2} \tag{21}$$

in the case of fixed singularities. The results change within a $\ln s$ factor for moving singularities. Some of these terms violate the **Froissant** bound and cannot therefore survive asymptotically.

It still remains to be seen experimentally whether the non-diffractive cross-section $\sigma_{n.d.}$ is constant in the very high energy regions and σ_I is responsible for the $\ln s$ increase. If that is not the case modifications like Eq. (21) may be expected in the observable energy ranges and analogous corrections will affect the distributions discussed in Section III.

III. PARTIAL CROSS-SECTIONS IN DIFFRACTIVE PROCESSES

Let us use the equations discussed in the previous section, in order to determine the distributions of n particle production in a diffractive process. These distributions depend strongly on the functional behavior of the Pomeron - the various functions denoted by B in the integral equations. We will use the Regge pole forms discussed above. Another crucial factor is the form of the generating function of the proper production processes. We choose to discuss a Poisson distribution, namely

$$\bar{Q}(s,z) = \sum_n \bar{\sigma}_n z^n = z^2 \bar{\sigma} \exp\{(2\alpha_R - 2 + Gz)\ln s\}$$
$$\bar{\sigma}_n = \bar{\sigma} \frac{(G\ln s)^{n-2}}{(n-2)!} s^{2\alpha_R - 2} \tag{22}$$

which is a simplified multiperipheral distribution for a chain dominated by the exchange of a fixed pole α_R.[10] The corresponding total cross-section will have a power dependence, $\bar{\sigma}(s) = \bar{\sigma} s^{\bar{\alpha}-1}$ where

$$\bar{\alpha} - 1 = 2\alpha_R - 2 + G \tag{23}$$

and the leading singularity of Fig. 1 is obtained for $\bar{\alpha} = 1$. We will nontheless leave $\bar{\alpha}$ free in order to see interesting effects that may be expected from large non-leading singularities. We will also comment on distributions which are different from Poisson.

Let us start with single diffraction, namely the mechanism we

denoted by I - the triple Pomeron. Using Eq. (6) we find for the n-particle cross-section (where n includes also the leading particle)

$$\sigma_{\tilde{n}M}(s,s_M) = \int_1^{s_M} \frac{d\sigma_{\tilde{n}M}(s,s_1)}{ds_1} ds_1 ; \quad \frac{d\sigma_{\tilde{n}M}}{ds_1} = \frac{1}{s_1} \frac{\beta^2 g}{16\pi^2} \frac{G^{\tilde{n}-3}}{(\tilde{n}-3)!} \frac{(\ln s_1)^{\tilde{n}-3} s_1^{2\alpha_R-2}}{2b+c+2\alpha' \ln(s/s_1)} \tag{24}$$

$\sigma_n(s,s_M)$ is a function of the total energy $\sqrt{s}$ and the upper limit of integration s_M. Since the triple-Pomeron representation is meaningful only over a limited region $x > 0.9$ or 0.85, we should correspondingly choose $s_M < 0.1\, s$ or $0.15\, s$.

We see from Eq. (24) that the s-dependence is at most logarithmic, as appropriate for a diffractively produced process. In the case $\alpha' = 0$ one obtains, upon performing the integration, the closed form

$$\sigma_{\tilde{n}} = \frac{\beta^2 g}{16\pi^2} \frac{\bar{\sigma}}{(2b+c)(2-2\alpha_R)} \left(1 - \frac{1-\bar{\alpha}}{2-2\alpha_R}\right)^{\tilde{n}-3} \frac{\gamma(\tilde{n}-2, (2-2\alpha_R)\ln s_M)}{(\tilde{n}-3)!} \tag{25}$$

where γ is the incomplete gamma function. This form can be approximated by

$$\sigma_n \to \begin{cases} \dfrac{\beta^2 g}{16\pi^2} \dfrac{\bar{\sigma}}{(2b+c)(2-2\alpha_R)} \left(1 - \dfrac{1-\bar{\alpha}}{2-2\alpha_R}\right)^{n-3} & \text{for } n-3 \ll (2-2\alpha_R)\ln s_M \\ \dfrac{\beta^2 g}{16\pi^2} \dfrac{\bar{\sigma}}{2b+c} G^{n-3} \dfrac{(\ln s_M)^{n-2}}{(n-2)!} s_M^{-(2-2\alpha_R)} & \text{for } n-3 \gg (2-2\alpha_R)\ln s_M \end{cases} \tag{26}$$

In Fig. 5 we show the results of a numerical evaluation of Eq. (24) using $\bar{\alpha} = 1$ for the two cases $\alpha' = .3$ and $\alpha' = 0$. σ_n are plotted vs.

$y_M = \ln s_M$. We note that for reasonable values of the parameters the $\alpha' = 0$ approximation is very good. Thus in Fig. 5a we note that since $Y = 7.3$ we obtain $y_M = 5$ by the restriction $x > 0.9$. In this range Fig. 5a is well approximated by Fig. 5b. The latter is independent of Y and shows the characteristics expected from the asymptotic approximations of Eq. (26) for $\bar{\alpha} = 1$, namely an asymptotic equality of the various σ_n (in the limit $n << y_M$) and a rapid fall off if $n >> y_M$. The fact that asymptotically all σ_n are equal is a property of the triple Pomeron amplitude and follows directly from the multiperipheral character that we assumed for the proper production amplitudes.[7,11] Thus if we change from a Poisson to a Gaussian distribution

$$\bar{\sigma}_n(s_1) = \frac{\bar{\sigma}}{D\sqrt{2\pi}} \; e^{-\frac{1}{2}\left(\frac{n-\bar{n}}{D}\right)^2} \tag{27}$$

and maintain the property $\bar{n}(s_1) = G \ln s_1$, we also find that the integrated multiplicity distribution in the PPP case is constant in n if $n << G \ln s_M - D(s_M)$. This means that the same result is obtained as long as the peak of the distribution (27) is well confined within the range of integration in Eq(24). At higher n values the multiplicity distributions fall rapidly because the integration of Eq. (24) will involve only the tail of the Gaussian distributions.

It is very easy to see qualitatively how this result comes about. The triple Regge formula leads to $\frac{d\sigma}{ds_1} \sim \frac{1}{s_1}$. If one makes the drastic

approximation $n = c \ln s_1$ one obtains $\sigma_n \equiv \frac{d\sigma}{dn} = \text{const.}$*** If one changes the $\ln s_1$ dependence to, say, $n = cs_1^{\epsilon}$ one obtains a mild decrease: $\sigma_n \propto \frac{1}{n}$.

At available NAL energies we are at $y_M \approx 4$. Fig. 5 shows us that the asymptotic form does not apply yet and, indeed, a variation of σ_n with n is observed experimentally[12] and looks very much like the structure of Fig. 5. However when looking at data we should not forget that in addition to the PPP production mode we may encounter other diffractive terms. We turn therefore to a brief discussion of the PPR case.

Using the same equations to describe a PPR production mode, we obtain from Eq. (26) an exponential damping in n by allowing $\bar{\alpha} < 1$. Hence we find that the PPR term contributes a constant diffractive structure which dies out quickly with n. This is the type of diffraction incorporated in many models[13] and is very different from the asymptotic constant pattern of PPP production discussed above. Once again one can reach this conclusion[11] by using the simplified model in which $n = c \ln s_1$. Since in the PPR amplitude $\frac{d\sigma}{ds_1} \sim s_1^{\bar{\alpha}-2}$ we see that $\sigma_n \sim s_1^{\bar{\alpha}-1} = e^{\frac{n}{c}(\bar{\alpha}-1)}$. Here we note that a big difference exists between $\ln s$ and power dependence since if $n = cs_1^{\epsilon}$ we obtain $\sigma_n \sim n^{(\frac{\bar{\alpha}-1}{\epsilon}-1)}$. In particular the nova model result[14] $\sigma_n \sim n^{-2}$ is obtained for $\bar{\alpha} = \epsilon = \frac{1}{2}$.

It is straightfoward to continue from single diffraction to double diffraction - case III. Using once again Eq. (23) for $\bar{Q}$ we obtain

$$\sigma_n^{III}(s) = \frac{1}{\pi^2}\,\frac{\beta^4 g^2}{(16\pi)^2}\cdot s^{2-2\alpha_R}\,\frac{G^{n-4}}{(n-4)!}\int_0^Y dy_1\,\frac{e^{-(2-2\alpha_R)y_1}}{2b+c+2\alpha'(Y-y_1)}\cdot$$

$$\cdot\int_{Y-y_1}^{Y} dy_2\,\frac{e^{-(2-2\alpha_R)y_2}}{2b+c+2\alpha'(Y-y_2)}\,(y_1+y_2-Y)^{n-4} \qquad (28)$$

which gives in the case $\alpha' = 0$

$$\frac{d\sigma_n^{III}}{ds_1} = \frac{A}{s_1}\left(\frac{G}{2-2\alpha_R}\right)^{n-4}\frac{1}{(n-4)!}\,\frac{1}{(2-2\alpha_R)}\,\gamma\,(n-3,\,(2-2\alpha_R)y_1) \qquad (29)$$

where $A = \frac{1}{\pi^2}\,\frac{\beta^4 g^2}{(16\pi)^2}\,\frac{1}{(2b+c)^2}$. This differential distribution shows of course the same character as the integrated distribution of Eq. (25). Once again one finds the asymptotic dependence or independence on n appearing if $\bar{\alpha}$ is smaller or equal to 1 respectively. Equation (28) can be integrated over the whole y_1 range to yield the generating function

$$Q^{III}(z) = A z^4\left\{\frac{e^{(2-2\alpha_R)(z\,a-1)Y}-1}{((za-1)(2-2\alpha_R))^2} - \frac{Y}{(za-1)(2-2\alpha_R)}\right\} \qquad (30)$$

(where $a = 1 - \frac{1-\bar{\alpha}}{2-2\alpha_R}$). Choosing now $\bar{\alpha} = 1$ and $\alpha_R = \frac{1}{2}$ one finds that this distribution has the following characteristics:

$$\langle n\rangle = \frac{1}{3}Y + 4 \qquad f_2 = \frac{1}{18}Y^2 - 4$$

These formulas for the moments change somewhat if one assumes $\alpha' \neq 0$ because the shape of the distribution changes. The important thing to test is therefore the variation of the distribution in n rather than the value of the corresponding moments.

It may be expected that double diffraction will be a negligible contribution to the total cross-section, as already remarked in the previous section. On the other hand the two jet production may be somewhat bigger. Let us examine the multiplicity distributions in this case (Fig. 2II). Using Poisson distributions for the proper amplitudes we find

$$\frac{d\sigma_n^{II}}{ds_1 ds_2} = \frac{1}{s_1 s_2} \cdot \frac{g^2\beta^2}{16\pi^3} \cdot \frac{G^{n-4}}{(n-4)!} \cdot \frac{(s_1 \cdot s_2)^{2\alpha_R - 2}}{2c + 2\alpha' \ln(s/s_1 s_2)} (\ln s_1 s_2)^{n-4} \qquad (31)$$

The variables s_1 and s_2 designate the $(\text{mass})^2$ of the two jets.

Using $\alpha' = 0$ one can simply integrate on one variable to obtain

$$\frac{d\sigma_n^{II}}{ds_1} = \frac{1}{s_1} \cdot \frac{g^2\beta^2}{16\pi^3} \cdot \frac{1}{2c} \cdot \frac{G^{n-4}}{(n-4)!} \sum_{\ell=2}^{n-2} \binom{n-4}{\ell-2} \frac{y_1^{n-\ell-2} s_1^{2\alpha_R - 2}}{(2-2\alpha_R)^{\ell-1}} \gamma(\ell-1, (2-2\alpha_R)(Y-y_1)$$

(32)

The form of $\frac{d\sigma_n}{dy_1} = s_1 \frac{d\sigma_n}{ds_1}$ is displayed in Fig. 6 which shows the results of a numerical integration of Eq. (31) using $\alpha' = .3$.

In Eq. (32) we observe that in the limit $y_1 \to 0$ only the term with $\ell = n - 2$ contributes. This leads to the same asymptotic intercept for all $d\sigma_n/dy_1$. Figure 6 displays this type of behavior for low n values. Note also that for low n one finds a concentration of the distribution year $y_1 \approx 0$ whereas for high n a broad plateau developes. This result is characteristic of the chain structure of the multiperipheral model. In the high y_1 region common dampting of $s_1^{2\alpha_R - 2}$ becomes important as can be seen in the figure.

In order to investigate experimentally the two-jet diffractive production one may select all exclusive events which show a rapidity gap which is bigger than some specified number Δ. For higher values of Δ (say 2 or 3) we have a high probability of finding diffractive events. After subtracting the elastic and single diffractive events one can look for the features of the two jet model. In plotting Fig. 6 we used an integration only up to $y_2 < Y - y_1 - \Delta$ where $\Delta = 2$. The effect of such a procedure on Eq. (32) is to replace $Y - y_1$ by $Y - y_1 - \Delta$ in the argument of the incomplete gamma-function.

Each of the two jets has characteristics similar to those seen in the jet of single diffractive production. Using the same simplifying argument as in the discussion after Eq. (27), we note that for $n << \ln s$ we find $d\sigma^{II}/dy_1 dy_2 \approx \sigma^{II}_{n_1, n_2} \approx$ const.*** Hence we should obtain $\sigma^{II}_n \sim n$

asymptotically, which leads to the $\ln^2 s$ increase of σ_{II} in Eq. (11). The curves of Fig. 6 indeed show an increase of σ_n with n for the low n values.

Finally we would like to make two remarks that concern all our results. The first is once again about the pole assumption. The formulas were derived for a moving pole with residues that were exponential functions of t. Most of the asymptotic results come actually from the $\alpha' = 0$ term. Changing from this picture to any other one, suitable modifications should occur. Thus if the triple Pomeron vertex decouples at $t = 0$ we have additional $\ln s$ denominators; nevertheless we expect the same qualitative results to emerge as long as the energy is not too big. Our equations show which results depend on the s-behavior of the Pomeron, and which reflect the character of the non-diffractive (proper) distributions. It is therefore straightforward to find the modifications that arise by changing these elements of the model. The second remark is that we did not try to distinguish between different kinds of particles. In order to connect our results to the measured cross-sections for, e.g., a fixed number of prongs, one has to add specific assumptions about the structure of the production process. Nevertheless the qualitative features such as the constant or power or exponential dependence on n should be strongly reflected also in the corresponding prong distributions.

As an example of this last point we present in Fig. 7 a comparison between recent diffractive pp data at $p_{lab} = 300$ GeV[12] and a very simplified model based on the PPP distribution of Eq. (24). Assuming that the outgoing particles are mainly two protons and equal numbers of the three kinds of pions we identify $n_c = \frac{2}{3}(n+1)$ and $\sigma_{n_c} = \sigma_{n-1} + \sigma_n + \sigma_{n+1}$. The resulting predictions are shown in Fig. 7 for the choice of parameters $Y = 6.3$, $\alpha' = .3$, $b = c = 2.5$ BeV^{-2}. The four and six prongs data are fitted perfectly. The 8 - 10 prongs lie somewhat higher than expected. This may reflect a deviation from the assumed Poisson input. The authors[12] quote an upper limit for the two prongs inelastic data at $x > 0.9$ ($y_M = 4$) of 1.1 ± 0.2 mb which can be well accommodated by this model. It is amazing how good a fit one can obtain without resorting even to a PPR component. We do not claim that this means that all simplifying assumptions that we made all along the way are thus proved to be correct. The complete picture of diffraction will presumably turn out to be much more complicated when all its details are revealed experimentally. Nevertheless the fact that it is easy to obtain such a good fit to the data is an indication that the theoretical expressions depict correctly the basic experimental trends.

APPENDIX

In the appendix we derive integral equations that can serve as a reformulation of a simplified multiperipheral model. The integral equations which we use in Chapter 2 are based on the same forms which we present here. The equations involve the generating function

$$Q(s,t) = \sum_n z^n \sigma_n(s) \tag{A-1}$$

which is normalized to the total cross-section $Q(s, z=1) = \sigma$. We will first discuss the derivation of the Bathe-Salpeter equation.

We start by assuming that the n-particle production amplitude (for simplicity we consider only one type of particles) is given by[11]

$$T_{2\to n}(p_1 p_2 \to q_1 \ldots q_n) = X_1(\frac{s}{s_1}, t)\, T_{2\to n-1}(p_1, p_1 - q \to q_2 \ldots q_n) + X_2(\frac{s}{s_0}, t)\, \delta_{n,2} \tag{A-2}$$

where $s_0 \approx 1\ \text{GeV}^2$ and $s_1 = (p_1+p_2-q_1)^2$. An example is

$$X_1(\frac{s}{s_1}, t) = \gamma(t)\,(\frac{s}{s_1})^{\alpha(t)}\rho(t) \qquad X_2(\frac{s}{s_0}, t) = \gamma(t)\,(\frac{s}{s_0})^{\alpha(t)}\gamma(t)$$

If $\alpha(t) = \alpha(0) + \alpha' t$ we have a multi-Regge model. The case $\alpha' = 0$ generates through s-channel unitarity a moving Regge pole in the two body scattering amplitude and if $\alpha' \neq 0$ one obtains a moving cut output.

s-channel unitarity connects the absorptive part of the two body amplitude

$$A(s,t) = \text{Im } T_{el}(s,t), \qquad A(s,o) = s\sigma \tag{A-3}$$

with the n-particle production amplitudes

$$A(s,t) = A_2(s,t) + \frac{1}{2}\sum_{n=3}^{\infty}\int d\Phi_n \; T_{2\to n}(p_1p_2\to q_1\ldots q_n)\, T^{*}_{2'\to n}(p_1'p_2'\to q_1\ldots q_n). \tag{A-4}$$

$A_2(s,t)$ is the contribution of the two particle (elastic) intermediate state

$$A_2(s,t) = \frac{1}{16\pi^2 s}\int \frac{dt_1 dt_2\;\theta(-\lambda)}{\sqrt{-\lambda(t_1,t_2,t)}}\; X_2(\frac{s}{s_0},t_1)\, X_2^{*}(\frac{s}{s_0},t_2) \tag{A-5}$$

Note that $T_{2\to 2}$ is determined by X_2 in Eq. (A-2) and is not identical with the resulting T_{el} whose imaginary part is determined by (A-4). We do not attempt to use here a bootstrap multiperipheral approach.

Let us denote the n-particle contribution to Eq. (A-4) by A_n:

$$A_n(s,t) = \frac{1}{\pi}\int \frac{ds_1}{s_1}\; B_I(\frac{s}{s_1},\, t)\, A_{n-1}(s,\, t) \tag{A-6}$$

where

$$B_I(s,t) = \frac{1}{16\pi^2 s}\int \frac{dt_1 dt_2}{\sqrt{-\lambda}}\; X_1(s,\, t_1)\, X_1^{*}(s,\, t_2) \tag{A-7}$$

The generating function is obtained by

$$Q = \sum_n z^n \sigma_n = \sum_n z^n \frac{1}{s}\, A_n(s,0) \tag{A-8}$$

and obeys therefore the equation

$$Q(s,z) = z^2\sigma_2 + \frac{z}{\pi s}\int_1^s ds_1\; B_I(\frac{s}{s_1},\, 0)\, Q(s_1,z) \tag{A-9}$$

In the fixed pole model

$$X_1(s,t) = \gamma(t)\,\rho(t)\,s^{\alpha_R} \qquad X_2(s,t) = \gamma^2(t)\,s^{\alpha_R} \tag{A-10}$$

we obtain

$$\sigma_2 = \frac{1}{s}A_2(s,0) = \frac{s^{2\alpha_R-2}}{16\pi}\int dt\,|\gamma(t)|^4 \equiv G_0 s^{2\alpha_R-2} \tag{A-11}$$

and Eq. (A-9) becomes

$$Q(s,t) = z^2\sigma_2 + \frac{zG_1}{\pi}\int_1^s \frac{ds_1}{s_1}\left(\frac{s}{s_1}\right)^{2\alpha_R-2} Q(s_1,z) \tag{A12}$$

where we used $\frac{B_I(s)}{s} = G_1 s^{2\alpha_R-2}$. This leads to the well known[10] Poisson distribution

$$\sigma_n(s) = G_0\,\frac{(\frac{G_1}{\pi}\ln s)^{n-2}}{(n-2)!}\,s^{2\alpha_R-2}$$

$$Q(s,z) = G_0 z^2 s^{2\alpha_R-2+zG_1/\pi} \tag{A-13}$$

It is straightforward to check that (A-13) is the solution to (A-12).

In looking for a formula for the description of the single diffractive mode, Fig. 2I, we used the same type of integral equation as (A-9). The corresponding formula is Eq. (2) that uses in B_I a Pomeron exchange, and builds the diffractive generating function Q_I from the non-diffractive $\overline{Q}$. The analogy of $\gamma(t)$ is $\beta(t)$ and corresponding to $\rho^2(t)$ one finds there $g(t)$. To establish the formulas for cases II and III let us look for alternative expressions to Eq. (A-9). An alternative approach can be obtained by starting with a fixed point of division into right and left in rapidity. For example, let us deal separately with particles produced

with either positive or negative c.m. rapidity whose invariant masses will be denoted by s_1 or s_2 respectively. If we try to develop an integral equation for the production of n-particles we realize that it has to be separated into the following terms: ${}^1_L{}^1_R$(for n=2), ${}^1_L(n-1)_R$, $(n-1)_R{}^1_L$, ${}^{n'}_R(n-n')_L$ for $n' \geq 2$. Here L and R denote left and right respectively. Using the same assumptions as before we can then write the following equation

$$Q(s,z) = z^2\sigma_2 + \frac{2z}{\pi s}\int_1^{\sqrt{s}} ds_1\, B_I(\frac{s}{s_1})Q(s_1,z) + \frac{1}{\pi^2 s}\int_1^{\sqrt{s}}\int_1^{\sqrt{s}} ds_1 ds_2\, B_{II}(\frac{s}{s_1 s_2})\cdot \tag{A-14}$$
$$\cdot Q(s_1,z)\,Q(s_2,z)$$

The last term corresponds to the production of two groups of particles whose corresponding (mass)^2 are s_1 and s_2 (notation as in Fig. 2II). B_I is the same function as defined above and B_{II} is similar but for the change $X_1 \to X_3 = \rho^2(t)s^{\alpha_R}$ in its definition (see Eq. (A-7)). The fixed pole model leads then to

$$Q(s,z) = z^2\sigma_2 + \frac{2zG_1}{\pi}\int_1^{\sqrt{s}} \frac{ds_1}{s_1}(\frac{s}{s_1})^{2\alpha_R-2} Q(s_1,z) + \frac{G_2}{\pi^2}\int_1^{\sqrt{s}}\int_1^{\sqrt{s}} \frac{ds_1}{s_1}\frac{ds_2}{s_2}\cdot \tag{A-15}$$
$$\cdot (\frac{s}{s_1 s_2})^{2\alpha_R-2} Q(s_1,z)\,Q(s_2,z)$$

where we used $\frac{B_{II}(s)}{s} = G_2 s^{2\alpha_R-2}$. Using the equality $G_2 = \frac{G_1^2}{G_0}$, expected from the definitions of the couplings given above, we find that the solution to Eq. (A-15) is indeed given by (A-12).

In order to derive such a second order equation in Q it is necessary to fix a division point in the double integral. The last term in Eq. (A-14) and (A-15) corresponds to an exchange between the two production amplitudes that is centered around $y_{c.m.} = 0$. If we were to integrate over the whole region $-\frac{Y}{2} \leq y_1 < y_2 \leq \frac{Y}{2}$ we would count the same diagram many times since the production amplitudes are built out of the same exchanges as the one appearing in B_{II}. This problem does not exist in Eq. (8) since the B_{II} there is built out of Pomeron exchange which does not appear in $\bar{Q}$. Otherwise Eq. (8) is of the same general character as the last term in (A-14).

Finally let us turn to a formulation of the same problem in a third way in which we insist on the separation into two leading particles and an intermediate production process. Using the notation of Fig. 2III and adding separately two- and three-particle production we obtain

$$Q(s,z) = z^2\sigma_2 + z^3\sigma_3 + \frac{z^2}{s^2\pi^2}\int_1^s\int_1^s \theta(s_1s_2 - s)\, ds_1 ds_2 B_I(\frac{s}{s_1})B_I(\frac{s}{s_2}) \cdot \cdot Q(\frac{s_1s_2}{s}, z) \tag{A-16}$$

The reasoning is the same that was used in the previous integral equation. The fixed pole limit leads to

$$Q(s,z) = z^2\sigma_2 + z^3\sigma_3 + \frac{z^2G_1^2}{\pi^2}\int_1^s\int_1^s \theta(s_1s_2 - s)\frac{ds_1}{s_1}\frac{ds_2}{s_2}(\frac{s}{s_1})^{2\alpha_R-2} \cdot (\frac{s}{s_2})^{2\alpha_R-2} Q(\frac{s_1s_2}{s}, z) \tag{A-17}$$

and, needless to say, Eq. (A-13) is the solution.

FOOTNOTES

*The name "two component model" is used in the terminology of multiparticle production theory to describe models[1] which have two separate production mechanisms (i.e., multiperipheral + diffractive). We use the same name, since we distinguish between proper and diffractive amplitudes. However we will identify more than two components in the partial cross-sections. Thus we will see that even the single particle diffraction process turns out to have different characteristics in a PPP and PPR mode, the first contributing to n particle production up to n ~ ln s while the second has a limiting structure in n.

**After completion of our work we became aware of three recent papers that advocate this approach and view the triple Pomeron amplitude as respondible for the ln s increase of the total cross-section at ISR energies.[6,7,8] See also discussions of this point in ref. 11.

***This prediction is slightly modified if $\alpha' \neq 0$ in an obvious way. Further modifications are to be expected for different types of Pomeron singularities.

REFERENCES

[1]K. Fialkowski, Phys. Lett. 41B, 379 (1972); 43B, 61 (1973); W. Frazer, R. Peccei, S. Pinsky and C.I. Tan, UCSD preprint. H. Harari and E. Rabinovici, Phys. Lett. 43B, 43 (1972). L. Van Hove, Phys. Lett. 43B, 65 (1973). C. Quigg and J. D. Jackson, NAL-THY-93 preprint 1972.

[2]L. Caneschi and A. Pignotti, Phys. Rev. Lett. 22, (1969). R. Peccei and A. Pignotti, Phys. Rev. Lett. 27, 1538 (1971). C.E. DeTar et al., Phys. Rev. D4, 906 (1971). H.D.I. Abarbanel, et al., Ann. Phys. 73, 156 (1972).

[3]J. Finkelstein and K. Kajantie, Phys. Lett. 26B, 305 (1968).

[4]G.F. Chew, Phys. Rev. D7, 934 (1973).

[5]M. Bishari and J. Koplik, Phys. Lett. B44, 175 (1973).

[6]D. Amati, L. Caneschi and M. Ciafaloni, CERN-TH-1676.

[7]W.R. Frazer and D.R. Snider, UCSD-10P10-126.

[8]A. Capella, M-S. Chen, M. Kugler and R.D. Peccei, SLAC-PUB-1241.

[9]U. Amaldi, et al., Phys. Lett. 44B, 112 (1973). J.C. Sens, invited paper at the Conference on Recent Advances in Particle Physics (1973). See also Ref. 1.

[10]G. Chew and A. Pignotti, Phys. Rev. Lett. 20, 1078 (1968);

G. Chew and A. Pignotti, Phys. Rev. 176, 2112 (1968).

[11] D. Horn and F. Zachariasen, Hadron Physics at Very High Energies, Benjamin ed., to be published.

[12] F. T. Dao et al., NAL-PUB-73/22; UCLA-1072.

[13] K. Wilson, Cornell preprint CLNS-131 (1971). M. Bander, Phys. Rev. D6, 164 (1972). See also Ref. 1.

[14] R.C. Hwa, Phys. Rev. Lett. 26, 1143 (1971). M. Jacob and R. Slansky, Phys. Lett. 37B, 408 (1971).

FIGURE CAPTIONS

Fig. 1. Generation of a Pomeron by proper production amplitudes.

Fig. 2. Three cases of diffractive production: I. Single diffraction, II. Two jet production, III. Double diffraction.

Fig. 3. Contribution of the three diffractive processes of Fig. 2 to the s-channel unitarity equation.

Fig. 4. s-channel unitarity.

Fig. 5. Numerical integration of Eq. (24). Choice of parameters $Y = 7.3$, $\alpha_R = 0.5$, $G = 1$ ($\bar{\alpha} = 1$), $b = c = 2.5\ \text{BeV}^{-1}$. Case a: $\alpha' = 0.3$, case b: $\alpha' = 0$ (Eq. (25)). Note that for low y_M the two figures have the same structure. For high y_M one observes in 5b the approach to the asymptotic value.

Fig. 6. Partial cross-sections in the two-jet model. Choice of parameters: $Y = 7.3$, $\alpha_R = 0.5$, $G = 1$ ($\bar{\alpha} = 1$), $\alpha' = .3$, $c = 2.5\ \text{BeV}^{-1}$, $\Delta = 2$.

Fig. 7. Comparison of a simple PPP model for single diffraction (see text) with recent 300 GeV data.[12]

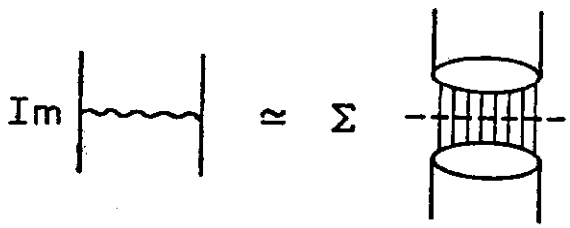

Figure 1

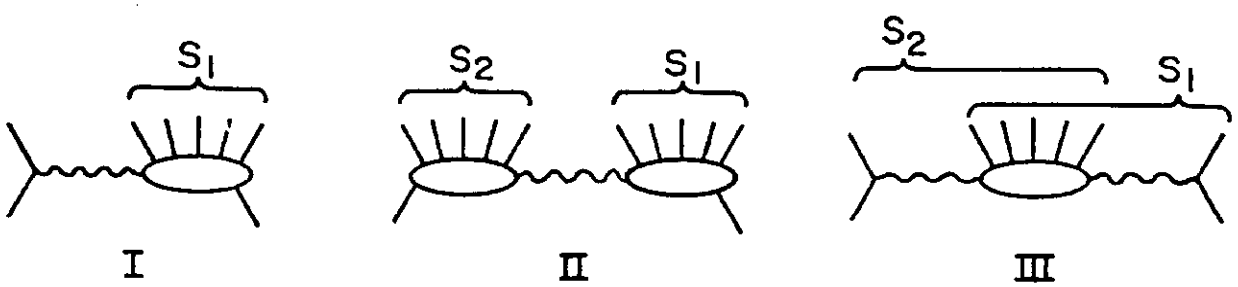

Figure 2

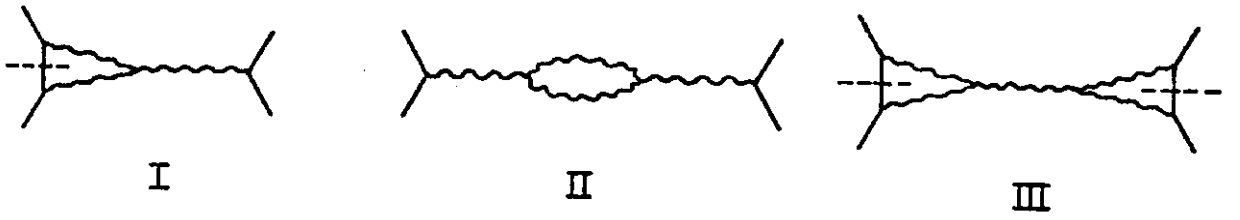

Figure 3

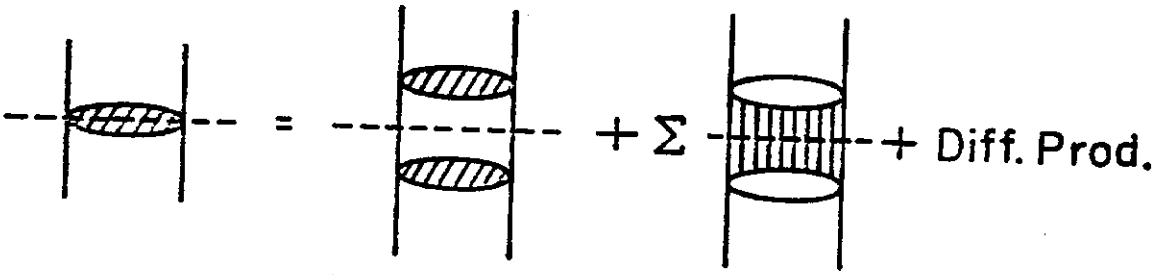

Figure 4

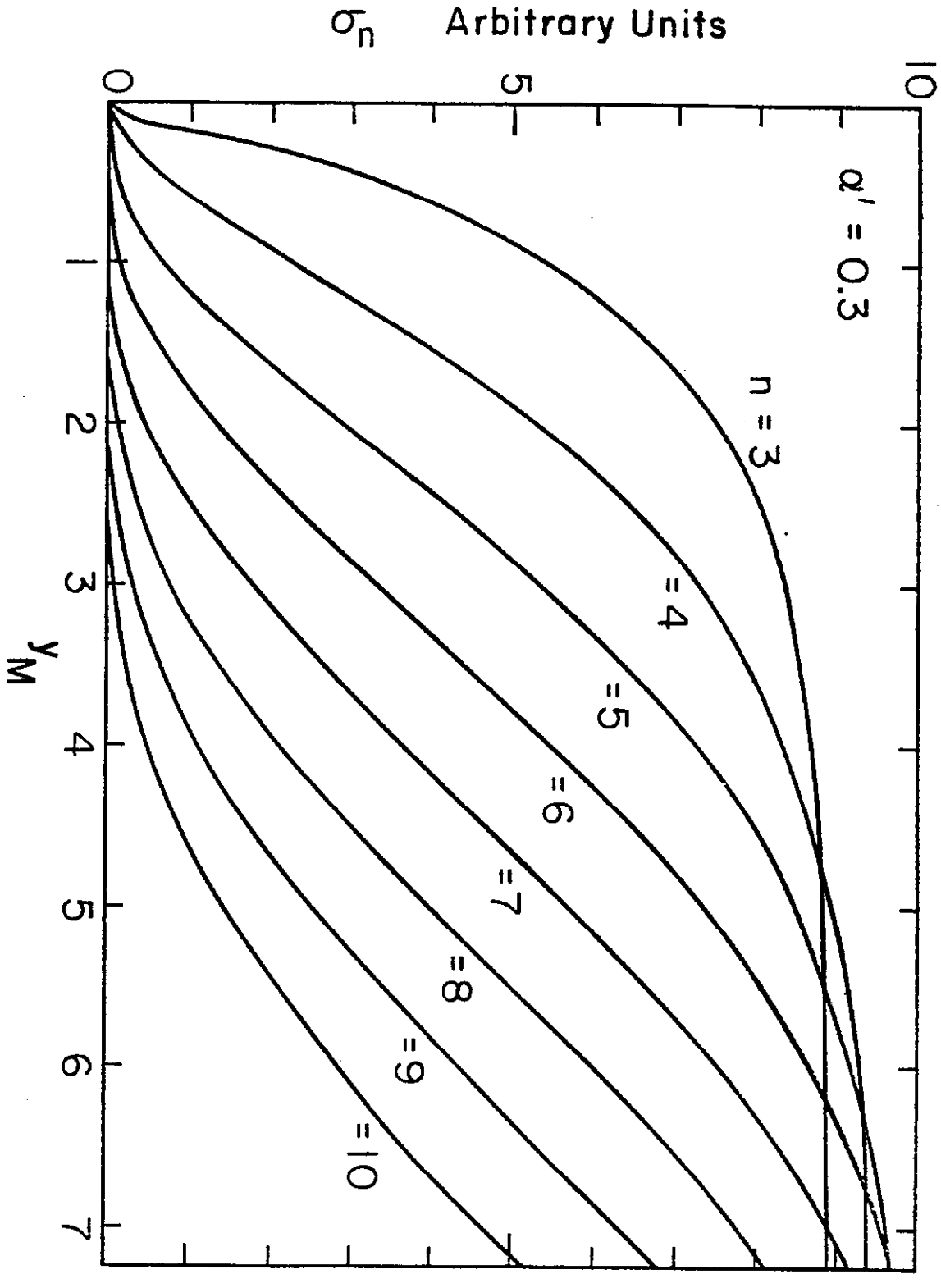
σ_n Arbitrary Units
0
5
10
$\alpha' = 0.3$
n = 3
=4
=5
=6
=7
=8
=9
=10
v_w
1
2
3
4
5
6
7

Figure 5a

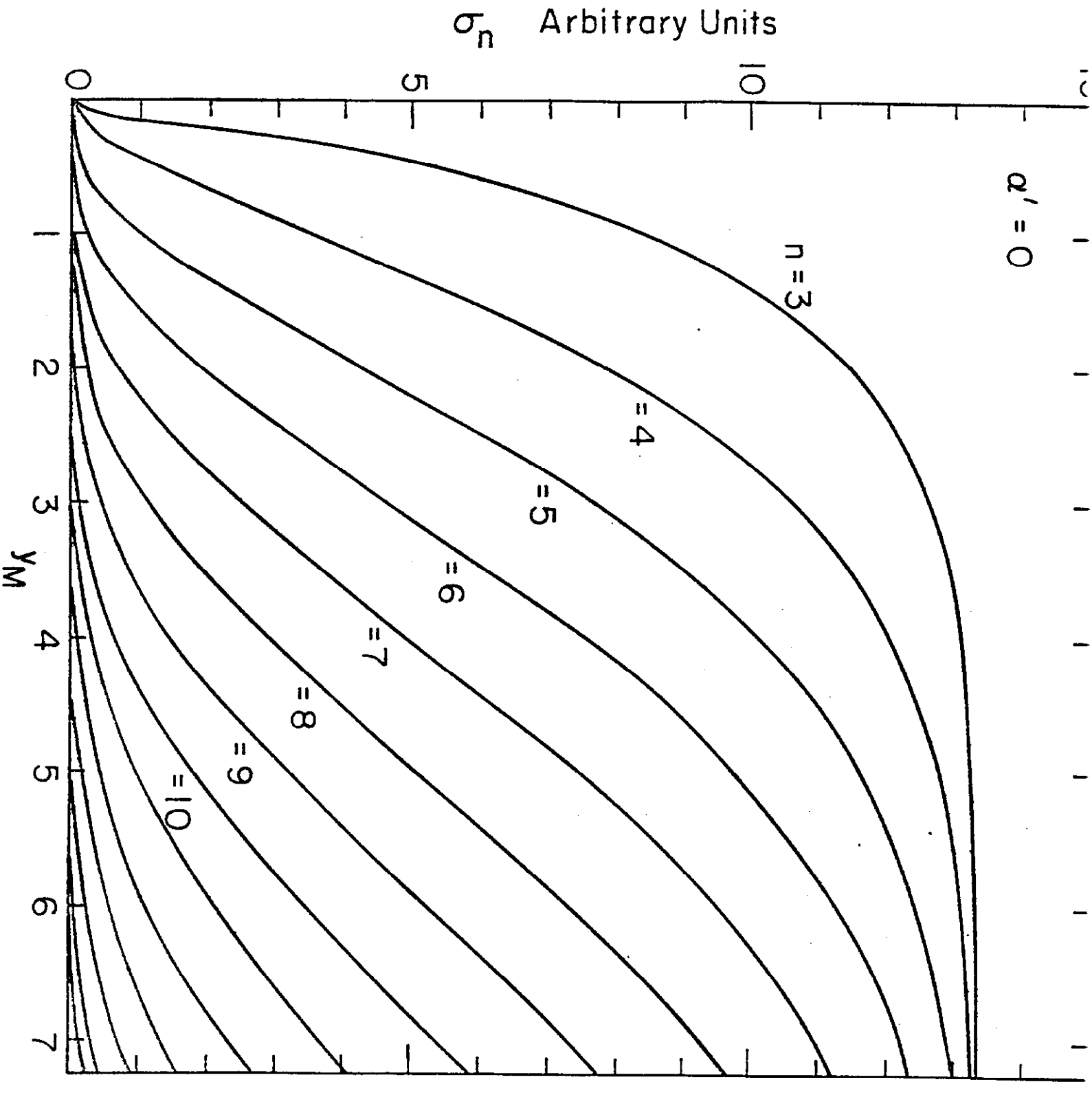

Figure 5b

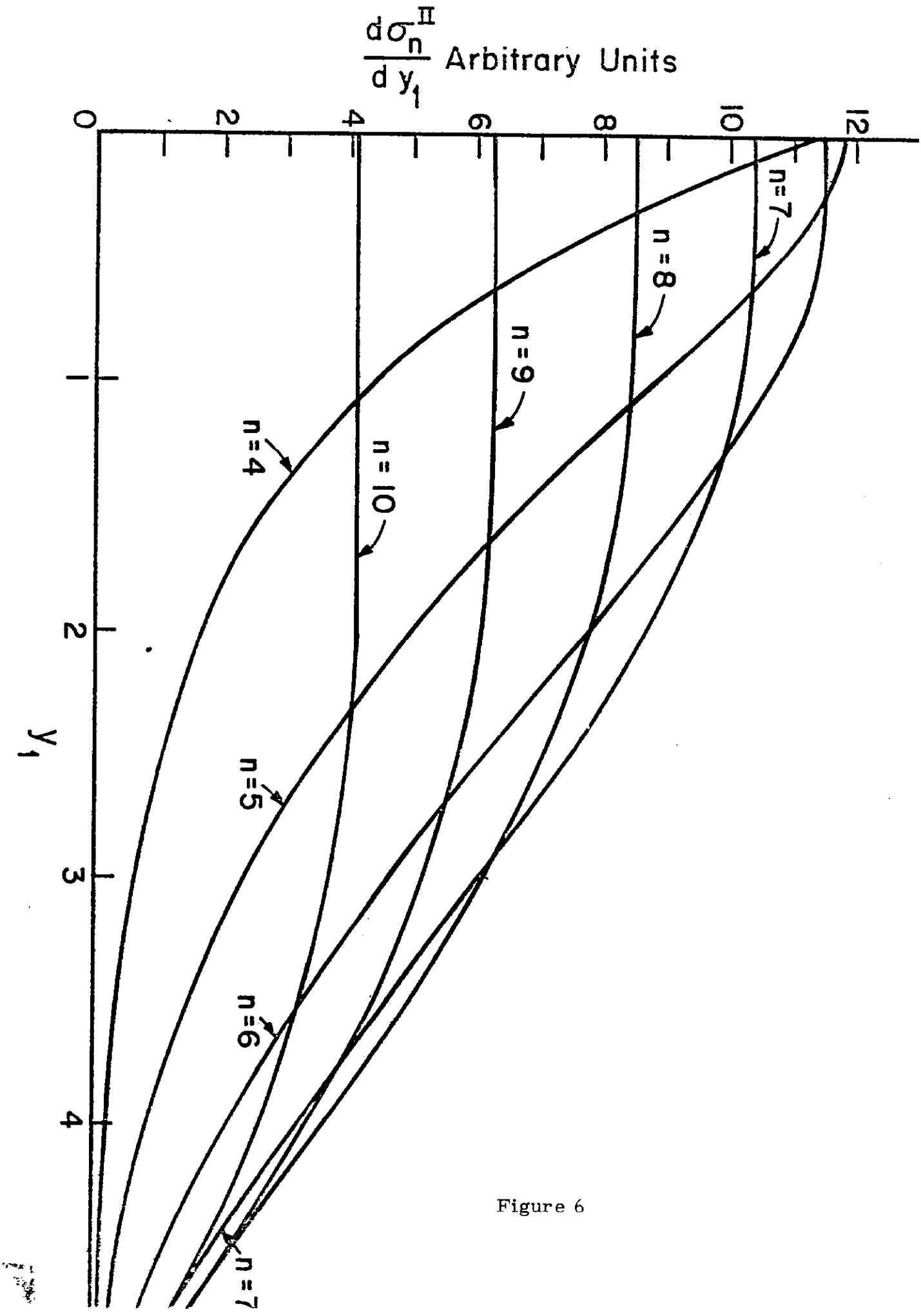
$\frac{d\sigma_n^{II}}{d y_1}$ Arbitrary Units
0
2
4
6
8
10
12
1
2
3
4
y_1
n=4
n=10
n=9
n=8
n=7
n=5
n=6
n=7

Figure 6

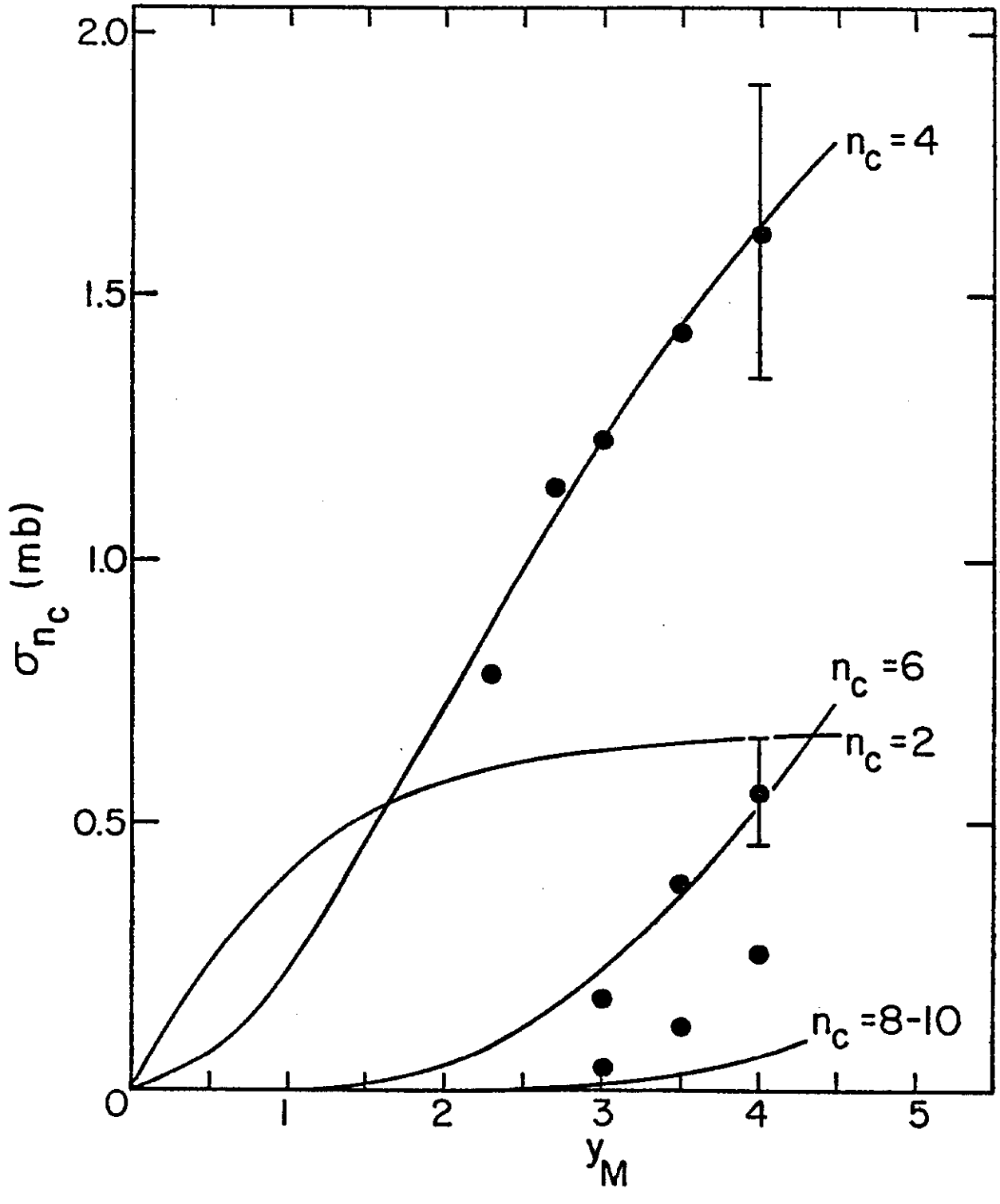

Figure 7